11-1-2015

Streambed and Water Profile Response to In-Channel Restoration Structures in a Laboratory Meandering Stream

Bangshuai Han
Boise State University

Hong-Hanh Chu
State University of New York

Theodore A. Endreny
State University of New York

AGU PUBLICATIONS

Water Resources Research

RESEARCH ARTICLE
10.1002/2015WR017177

Streambed and water profile response to in-channel restoration structures in a laboratory meandering stream

Bangshuai Han[1,2], Hong-Hanh Chu[1], and Theodore A. Endreny[1]

[1]Department of Environmental Resources Engineering, College of Environmental Science and Forestry, State University of New York, Syracuse, New York, USA, [2]Now at Department of Geosciences, Boise State University, Boise, Idaho, USA

Key Points:
- Restoration structures installed in a laboratory meandering river
- Detailed measurement on water and streambed profiles with and without structures
- Inform the design of stream restoration projects and/or structures

Correspondence to:
B. Han,
bangshuaihan@gmail.com

Citation:
Han, B., H.-H. Chu, and T. A. Endreny (2015), Streambed and water profile response to in-channel restoration structures in a laboratory meandering stream, *Water Resour. Res.*, *51*, 9312–9324, doi:10.1002/2015WR017177.

Received 28 FEB 2015
Accepted 12 NOV 2015
Accepted article online 18 NOV 2015
Published online 28 NOV 2015

Abstract In-channel structures are often installed in alluvial rivers during restoration to steer currents, but they also modify the streambed morphology and water surface profile, and alter hydraulic gradients driving ecologically important hyporheic exchange. Although river features before and after restoration need to be compared, few studies have collected detailed observations to facilitate this comparison. We created a laboratory mobile-bed alluvial meandering river and collected detailed measurements in the highly sinuous meander before and after installation of in-channel structures, which included one cross vane and six J-hooks situated along 1 bar unit. Measurements of streambed and water surface elevation with sub-millimeter vertical accuracy and horizontal resolution were obtained using close-range photogrammetry. Compared to the smooth gradually varied water surface profile for control runs without structures, the structures created rapidly varied flow with subcritical to supercritical flow transitions, as well as backwater and forced-morphology pools, which increased volumetric storage by 74% in the entire stream reach. The J-hooks, located along the outer bank of the meander bend and downstream of the cross vane, created stepwise patterns in the streambed and water surface longitudinal profiles. The pooling of water behind the cross vane increased the hydraulic gradient across the meander neck by 1% and increased local groundwater gradients by 4%, with smaller increases across other transects through the intrameander zone. Scour pools developed downstream of the cross vane and around the J-hooks situated near the meander apex. In-channel structures significantly changed meander bend hydraulic gradients, and the detailed streambed and water surface 3-D maps provide valuable data for computational modeling of changes to hyporheic exchange.

1. Introduction

Streambed morphology and stream water surface profile control hydraulic characteristics including stream depth, which in turn influence hydraulic gradients and the mixing of surface water and groundwater in and adjacent to the streambed. The mixing of these two water sources is termed hyporheic exchange flux, and defines the hyporheic zone which supports critical ecological and biophysical processes [*Boulton et al.*, 1998; *Cardenas et al.*, 2004; *Elliott and Brooks*, 1997; *Hester and Doyle*, 2008; *Packman and Brooks*, 2001]. Hyporheic exchange flux could be categorized into vertical exchange and lateral exchange [*Hester and Gooseff*, 2010]. Vertical exchange is primarily driven by the in-stream hydraulic head distribution, which is largely organized by surface water profiles and controlled by streambed geomorphology such as step-pool and riffle-pool sequences [*Kasahara and Wondzell*, 2003]. Lateral exchange is driven by the hydraulic gradient between the upstream bank and the downstream bank [*Gomez et al.*, 2012]. Lateral exchange is most commonly observed in meandering rivers with river water entering the upstream face of the intrameander zone and returning to the river through the downstream face of that intrameander zone [*Boano et al.*, 2006; *Han and Endreny*, 2013; *Revelli et al.*, 2008]. Measurement and evaluation of how restoration changes streambed morphology and stream water surface profiles are needed to better understand how restoration can increase beneficial ecological and biogeochemical processes in the hyporheic zone.

Streambed morphology and stream water surface profiles have been studied using computational simulations, field experiments, and more widely, a combination of these approaches. The computational simulation approach uses principles in fluid mechanics such as the continuity and momentum equations for the fluids, e.g., Reynolds equations, and principles in geomorphology such as the evolution equation for bed

topography, e.g., Exner equation. Solutions to these simulations may reproduce many of the main features of river channel flows, including the bed-generated turbulence features, lateral shear turbulence, and secondary flows, and may predict future river evolution [*Zolezzi and Seminara*, 2001]. Many empirical formulas are also used in the computational approach to close numerical solutions. Both analytical solutions and validated numerical solutions typically simplify the natural system [*Ikeda et al*., 1981; *Parker*, 1976; *Wu*, 2008]. Field experiments directly apply to the natural system, but are typically more expensive, time consuming, and difficult to replicate than computational models. Laboratory experiments, despite limitations in spatial and temporal scaling, provide a bridge between the commonly employed field experiment and computational simulation approaches, and are becoming popular in recent decades for studying river hydrodynamics [*Dijk et al*., 2012; *Schumm and Khan*, 1972; *Smith*, 1998] and facilitating physical tests more quickly [*Han and Endreny*, 2014b; *Ikeda et al*., 1981; *Peakall et al*., 1996]. Laboratory experiments provide a strategic approach to measure and assess how streambed morphology and water surface profiles are changed by stream restoration.

In-channel structures are used to deflect streamflow off the bank and stabilize the channel in river restoration [*Abad et al*., 2008; *Radspinner et al*., 2010]. Two common structures used in natural channel design include J-hook and cross vane [*Rosgen*, 2006], which are typically built with boulders. By steering river currents, these in-channel structures will likely change streambed morphology and stream water surface profiles, and thereby impact hydraulic gradients and the hyporheic exchange flux critical to many riverine ecosystems [*Doll et al*., 2003; *Stanford and Ward*, 1988]. Despite the controversy surrounding the extensive deployment of these natural channel design in-channel structures [*Endreny and Backer*, 2013; *Lave*, 2009; *Rosgen*, 2011; *Simon et al*., 2007; *Small and Doyle*, 2011], billions of dollars are currently spent restoring streams and rivers [*Palmer et al*., 2005; *Bernhardt and Palmer*, 2011]. However, detailed observations are lacking on how the structures change the hydraulic gradient driving hyporheic exchange [*Lehr et al*., 2015; *Zimmer and Lautz*, 2015], with most studies obtaining data after installation [*Crispell and Endreny*, 2009; *Smidt et al*., 2014]. Before and after restoration monitoring is preferred because it can isolate the effect of the structure as a treatment, and thereby allows restoration teams to establish design goals related to hydraulic gradients, hyporheic exchange, and ecological services [*Bernhardt et al*., 2005; *Jenkinson et al*., 2006; *Kondolf and Micheli*, 1995; *Radspinner et al*., 2010]. Laboratory monitoring can facilitate faster and replicable measurement of streambed morphology and water surface profiles with and without in-channel structures, and is utilized in this research.

In this research, we present a laboratory study that monitored how J-hook and cross-vane in-channel restoration structures impacted water surface and streambed profiles around a meander bend. These variables regulated the hydraulic head distribution along the meander bank and bed, and drove patterns and rates of vertical and lateral hyporheic exchange.

2. Methods and Materials

2.1. Laboratory Experiment Setup

Laboratory experiments were conducted on a mobile-bed sandbox river table with dimensions of 3.7 m × 1.8 m × 0.3 m and a recirculating water system, mostly the same as described in *Han and Endreny* [2014b] (Figure 1). We built a broad floodplain in the river table using homogenous mixture of fine sand and clay mediums ($D_{50} = 0.18$ mm) with an average porosity of 0.29. The physical layout of the design was selected to mimic a highly sinuous river, e.g., an "E" stream type in the Rosgen stream classification system [*Rosgen*, 1994]. The initial condition of the setup is detailed in the following. The floodplain had a slope of 1.8%, and was bounded by an upstream and a downstream water reservoir and a confining layer at the bottom which varies from 6.5 to 11.5 cm below the sand surface. We carved into the floodplain a single thread, flat-bed stream channel with three meander bends, 0.9% channel slope, 1.9 sinuosity, 14 cm average bankfull width, and 1.5 cm average bankfull depth (Figure 2). The first and third stream meander bends buffered the second meander bend from upper and lower stream boundary conditions. The study reach was the second stream meander bend from S to S′ (one meander wavelength) with a length of 2.2 m, approximately 16 channel widths (Figure 3). We installed 19 wells throughout the intrameander zone of our stream reach and in the nearby floodplain to monitor water table levels (Figure 3). The wells were mesh cylinders constructed from 50 × 50 galvanized steel mesh (0.37 mm mesh opening) with a diameter of 4.5 or 6.5 cm, and

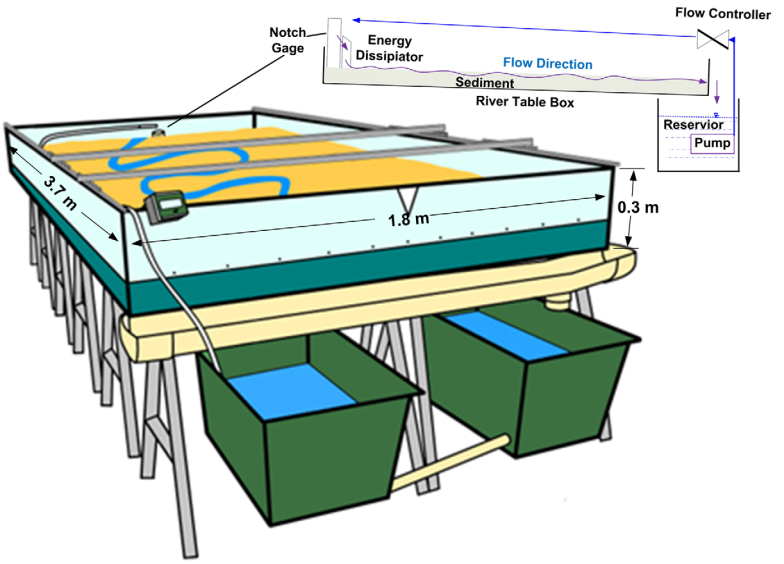

Figure 1. Illustration of the mobile-bed river table with a digital flow controller, downstream V-notch weir, groundwater discharge holes, recirculating water system, and rails for mounting and sliding equipment over the table.

extended from the top of the floodplain surface to the confining layer (i.e., river table surface). The average saturated hydraulic conductivity in the intrameander zone was 0.23 cm/h. A calibrated digital flow controller continuously discharged steady, nonuniform flow at 51 mL/s, which filled approximately 30% of channel capacity.

The experiments were run with streamflow at approximately 30% channel capacity, instead of at bankfull flow, in order to evaluate the streambed and water profile responses to a more frequently occurring effective discharge in our study [*Doyle et al*., 2007]. This setup also avoided frequent flooding which was not the aim of this study. To capture the stream stage and water table level, we added a thin layer of white wax powder (∼0.3 mm average diameter) on the surface of the stream and well water, and took digital photographs of the stream channel with 2 NIKON D5100 digital cameras mounted 1.3 m from the floodplain surface. The digital cameras also photographed the stream channel and floodplain before and after 7 h of flow during each experimental run. The channel was drained for at least 24 h after 7 h of continuous flow, photographed, and then reformed to initial conditions before starting each new experimental run. We repeated the experiment three times for a channel without in-channel restoration structures (control group) and four times for a channel with structures under the same initial conditions. We installed six J-hook vanes (J1, J2, J3, J4, J5, and J6) and one cross vane in the channel of our stream reach during the "with structures" experimental runs (Figure 3). The J-hooks were installed to protect the bank that experienced scouring under high streamflow during preliminary experiments [*Rosgen*, 2011]. The cross vane was installed to replicate the popular practice of forcing heterogeneous streambed topography and creating fish habitat in stream restoration [*Gordon et al*., 2013]. The model restoration structures were formed from gravels (1 cm

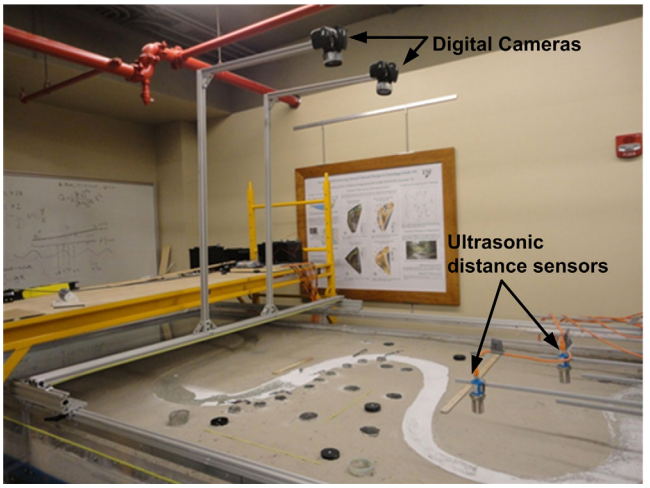

Figure 2. A picture showing the river table setup of experiments without in-channel restoration structures. Black circular structures are elevation control points. Grey cylindrical structures are water table wells.

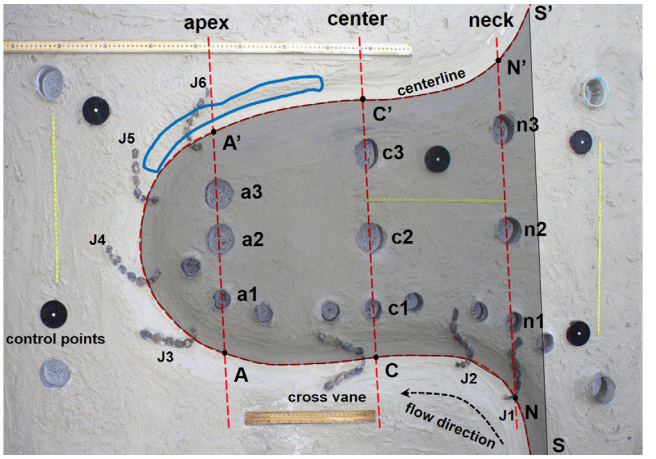

Figure 3. Rosgen style J-hooks and a cross vane were installed in the stream channel during the "with structures" experimental runs. Dashed lines indicate location of cross sections for water surface profile and hydraulic gradient analyses. Shaded area is the intrameander zone. The area outlined in blue downstream of the fifth J-hook (J5) was analyzed for significant bank erosion and deposition.

average diameter) held together by hot melt adhesive. The average full height of the structures (i.e., exposed and keyed areas) was 3 cm at the head end and 5 cm at the tail end. Footer depth ranged from up to 2 cm at the head end and up to 3.5 cm at the tail end of the structure. The slope of the J-hook arms was set to approximately 17%, and the slope of the cross-vane arms was set to approximately 10%. These values are larger than common practices in field restoration projects [*Rosgen*, 2006], but are necessary to induce sufficient hydrodynamic differences for observation in the small-scale experiment while mimicking natural restoration structures.

2.2. Data Processing

Digital photographs were processed in 3DM Analyst, a digital photogrammetric software by ADAM Technology that extracts 3-D data from digital photographs and creates digital elevation model (DEM) points. The steps taken to obtain DEM points are referenced in *Han and Endreny* [2014a]. All elevation values were referenced to the elevation of five control points (Figure 2), which were surveyed using SICK UM30-21113 ultrasonic distance sensors with an accuracy of up to 0.3 mm. The overall DEM accuracy and precision were tested to be within a millimeter, and can satisfy current laboratory analysis needs [*Han and Endreny*, 2014a]. We converted the DEM points into triangulated irregular network (TIN) surfaces and then into raster images with 1 × 1 mm in ESRI ArcMap.

2.3. Data Analysis

2.3.1. Streamwise Water Surface Analysis

Streamwise water surface profile and the slope of the stream channel centerline (S to S′) were extracted. The average slope of the streamwise water surface along the stream centerline was calculated for each replication. The water surface profile for all replications was averaged and plotted for analysis without losing important features of each replication due to the negligible variance between replications (Figure 4).

2.3.2. Intrameander Hydraulic Gradients and Cross-Sectional Water Table Profiles

Cross-sectional water table profiles were extracted at three transects (i.e., meander apex AA′, center CC′, and neck NN′ following *Han and Endreny* [2014b]) in the intrameander zone, and the hydraulic gradients

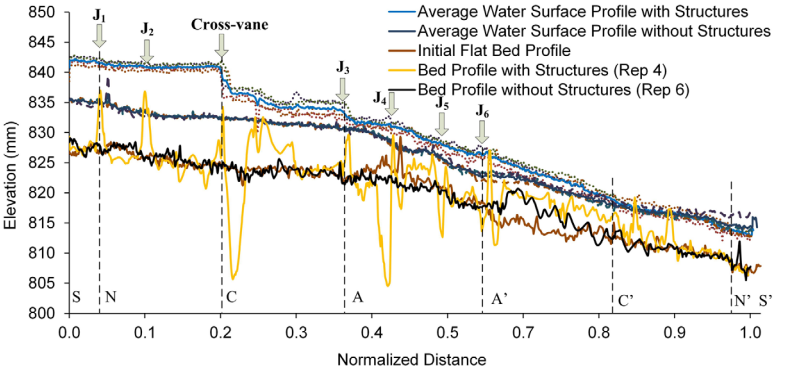

Figure 4. Streamwise water and bed surface profiles along the channel centerline (S to S′). Water surface profiles from each replicate are represented by dotted thinner lines. To make the figure clearer, we do not include all bed profiles due to their larger variance but similar trend. Instead, sample bed profiles (initial bed, Replication 4 representing bed profiles with structures and Replication 6 representing bed profiles without structures) are also denoted as solid lines as shown in the legend. The locations of J-hooks and cross vane are marked.

across these transects were calculated (Figure 3). To facilitate analysis, the wells installed in the intrameander zone were denoted as n1, n2, and n3 at the meander neck transect from upstream to downstream and similar nomenclature for c1, c2, and c3 at the meander center and a1, a2, and a3 at the meander apex (Figure 3).

We performed split-plot 2 × 3 factorial ANOVA tests for statistical significance in the intrameander hydraulic gradients and water table levels. The whole plot treatment levels were with structures and without structures. The subplot treatment levels were well water level and hydraulic gradient values at the meander neck, center, and apex. We ran an ANOVA test first for the water level increases in wells n1, c1, and a1. The well water level increases were determined as follows:

$$\Delta\overline{W} = \overline{W_S} - \overline{W_C} \tag{1}$$

where, $\Delta\overline{W}$ is the well water level difference, $\overline{W_S}$ is the well water level averaged across replicates with structures, and $\overline{W_C}$ is the well water level averaged across replicates without structures (control group). We repeated the same test for the replicate-averaged water level increases in wells at the middle (n2, c2, and a2) and downstream of the intrameander zone (n3, c3, and a3). We also ran ANOVA test for replicate-averaged increases in the hydraulic gradients across the intrameander zone along the three transects. The intrameander hydraulic gradients $HG_{NN'}$, $HG_{CC'}$, and $HG_{AA'}$ were determined as the quotient of the elevation difference between two points divided by the distance between the two points, and are shown in equations as follows:

$$HG_{NN'} = (\overline{Y_N} - \overline{Y_{N'}})/X_{NN'} \tag{2}$$

$$HG_{CC'} = (\overline{Y_C} - \overline{Y_{C'}})/X_{CC'} \tag{3}$$

$$HG_{AA'} = (\overline{Y_A} - \overline{Y_{A'}})/X_{AA'} \tag{4}$$

where, $X_{NN'}$, $X_{CC'}$, and $X_{AA'}$ denote the distance between the points at NN′, CC′, and AA′, and $\overline{Y_N}$, $\overline{Y_{N'}}$, $\overline{Y_C}$, $\overline{Y_{C'}}$, $\overline{Y_A}$, and $\overline{Y_{A'}}$ denote the stream water surface elevation averaged across replicates at each point. Hydraulic gradient increases were calculated in the same manner as the well water level increases, and the equation can be denoted as follows:

$$\Delta\overline{HG} = \overline{HG_S} - \overline{HG_C} \tag{5}$$

where, $\Delta\overline{HG}$ is the hydraulic gradient difference, $\overline{HG_S}$ is the hydraulic gradient averaged across replicates with structures, and $\overline{HG_C}$ is the hydraulic gradient averaged across replicates without structures (control group). Note that equation (5) as well as equation (1) are written as a general form, and apply to each transect at NN′, CC′, and AA′.

2.3.3. Forced Channel Morphology

Several important geomorphology features were analyzed for the experiments with and without structures. In each replicate, water depth was calculated from the difference in elevation between the stream surface and the channel bed surface. The volume of stream water was summed using the data of water depth and the area in each DEM grid. Erosion and deposition depths were calculated using the difference in elevation between the initial channel bed and the resulting channel bed after 7 h of continuous flow. The erosion and deposition volumes were calculated using the sum of erosion or deposition depth for all raster stream cells and the cell area.

We ran a two-sample Student's *t* test on the erosion and deposition volumes at an outer meander bend downstream of the restoration structures (at J5, J6, and downstream of J6 as shown in Figure 3) to test if the mean volume change is significantly different between scenarios with structures and without structures.

3. Results

3.1. Streamwise Water Surface Profile and Slope of the Channel Centerline

The streamwise water surface profile was changed by in-channel restoration structures from a single gradually varied condition to a series of rapidly varied transitions at each restoration structure (Figure 4). The

Table 1. Average Water Level Increase $\Delta\overline{W}$ (mm) by Installing Structures in the Stream Channel[a]

Meander Location	Upstream of Intrameander Zone	Intrameander Zone			Downstream of Intrameander Zone
Neck	6.7 (N)	2.1[b] (n1)	0.8[c] (n2)	0.3[c] (n3)	−0.8 (N′)
Center	8.6 (C)	3.8[b] (c1)	1.7[c] (c2)	0.2[c] (c3)	0.7 (C′)
Apex	3.0 (A)	0.5[b] (a1)	1.0[c] (a2)	1.2[c] (a3)	2.4 (A′)

[a]Values without [b] or [c] mean no significant change between with-structures groups and without-structures groups.
[b]Statistically significant increase across meander locations (neck, center, and apex) and between channel types (with structures, without structures) at $\alpha = 0.05$.
[c]Statistically significant increase across meander locations (neck, center, and apex) at $\alpha = 0.05$.

gradually varied water surface profile was a relatively deep and slow subcritical flow condition without structures, while the rapidly varied profile had transitions from subcritical to critical flow across the crest of the structure, characterized by a stepwise pattern. The cross vane caused an average local head loss (i.e., vertical drop in the water surface profile) of 4.6 mm, which counted for 16% of the total head loss in the entire stream reach (S to S′). The cross vane also produced backwater that flattened the upstream water surface profile for at least five channel widths and submerged the two J-hooks at the upstream meander neck. The first J-hook (J3) at the meander apex caused an average local head loss of 2 mm, which counted for 6.5% of the total head loss in the entire stream reach (S to S′) and flattened the upstream water surface profile for only two channel widths. Other J-hooks at the meander apex did not produce observable backwater or local head loss.

The average slope of the streamwise water surface in the entire stream reach (S to S′) increased from 1.0% to 1.4% after installing the in-channel structures. Stream stage increased approximately 6.7, 8.6, and 3.0 mm at the upstream side of the meander neck (N), center (C), and apex (A), respectively (Table 1). The stream stage also increased approximately 2.4 mm immediately downstream of the last meander apex J-hook (A′). The stream stage of channels with and without structures did not significantly differ at C′ or N′.

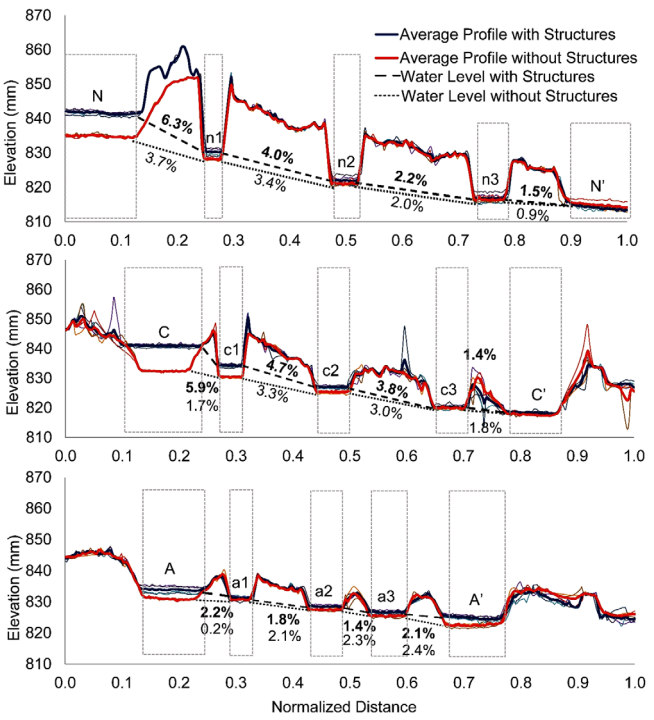

Figure 5. Cross section of the meander (top) neck, (middle) center, and (bottom) apex. Thick colored lines represent the cross-sectional surface profiles, includes both sand and water surface along a transect, averaged across replications. Thin colored lines denote the profile of each single replication. Intrameander hydraulic gradients are given and represented by black dashed lines with bold numbers (with structures) and dotted lines with plain numbers (without structures). Note that the horizontal axis is normalized distance for each cross section, and their real distances are different. Stream and well water surface elevations are enclosed in grey dashed boxes, but ground elevation is not.

3.2. Intrameander Hydraulic Gradients and Cross-Sectional Water Table Profiles

Hydraulic gradients across the intrameander zone increased more significantly with in-channel structures, especially at the meander neck and center (Figure 5). The average hydraulic gradient across the meander neck, center, and apex increased by 1.0%, 1.4%, and 0.2%, respectively, after in-channel structures were installed (Table 2). The difference was statistically significant across meander locations (neck, center, and apex) ($p < 0.0001$) and between channel types (with structures and without structures) ($p = 0.0002$). The restoration structures changed the intrameander hydraulic gradients disproportionately across meander locations ($p < 0.0001$).

Table 2. Hydraulic Gradient (mm/mm) Values Across the Intrameander Zone

Channel Type	$HG_{NN'}$ (Neck)	$HG_{CC'}$ (Center)	$HG_{AA'}$(Apex)
With structures	3.5%	4.0%	2.0%
No structures	2.5%	2.6%	1.8%
Difference	1.0%[a]	1.4%[a]	0.2%[a]

[a]Statistically significant difference across meander locations (neck, center, and apex) and between channel types (with structures, without structures) at $\alpha = 0.05$.

Water table levels in the observational wells throughout the intrameander zone were elevated after in-channel structures were installed, especially in the upstream half of the intrameander zone (Table 1). The average increase in the well water level at the upstream side of the intrameander zone (n1, c1, and a1) was statistically significant across meander locations (neck, center, and apex) ($p < 0.0001$) and between channel types (with structures, without structures) ($p = 0.0057$). The average increase in well water level at the middle (n2, c2, and a2) and downstream (n3, c3, and a3) of the intrameander zone was statistically significant across meander locations (neck, center, and apex) ($p < 0.0001$), but not statistically significant between channel types (with structures and without structures) ($p = 0.0797$).

Water table profiles in the intrameander zone also increased due to the elevated stream stage, especially at the upstream section (Figure 5). The gradient of the water table profile was steepest at the meander neck (near Well n1), e.g., 3.7% in the without-structures scenario and 6.3% in the with-structures scenario. However, the steepest increase of the water table profile was at the meander center (i.e., near the cross vane and Well c1), increasing from 1.7% to 5.9%. The effects of in-channel structures on the intrameander water table became less pronounced in wells located further from the structures. There was no significant change to the slope of the water table profile across the meander apex.

3.3. Forced Channel Morphology

Channel bed profiles changed more significantly with in-channel restoration structures than without structures (Figure 4). The spatial patterns of bed and bank erosion and deposition were similar among channels with structures (Figure 6). Scour pools developed downstream of the cross vane, and mostly around the hooked tip of the four meander apex J-hooks. The scour pool downstream of the cross vane had an average depth of 33.8 mm, and was the deepest of all scour pools in channels with structures (Table 3). The second

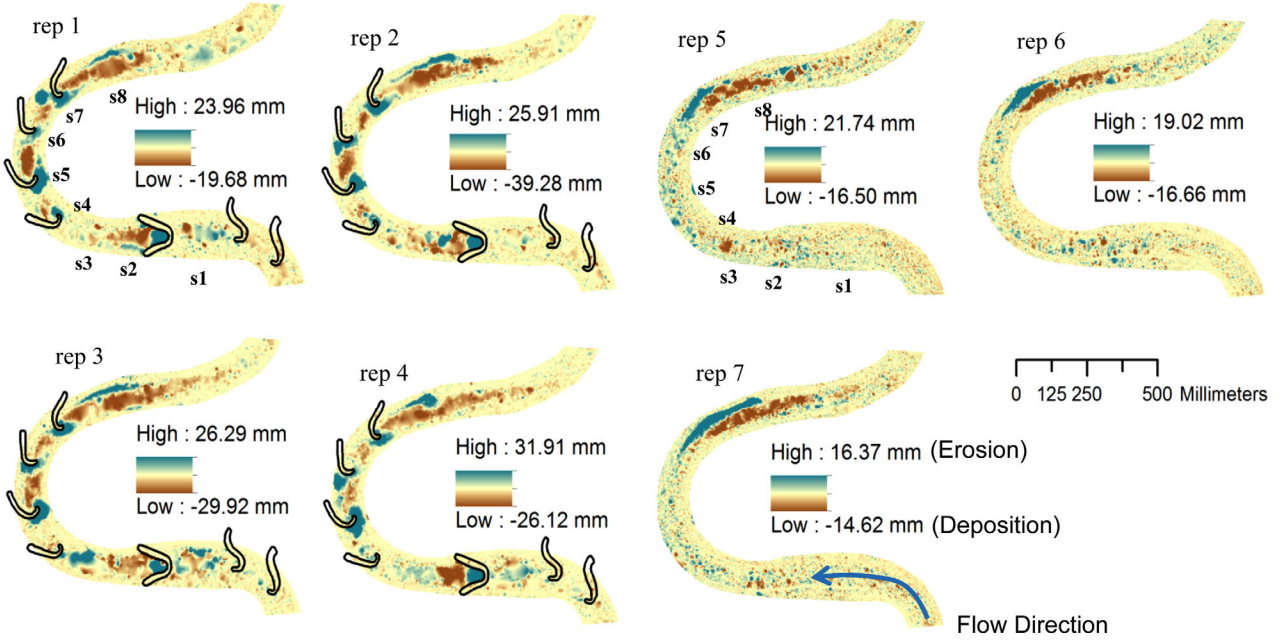

Figure 6. Raster images of the spatial distribution of channel bed and bank erosion (blue) and deposition (brown) after 7 h of continuous flow in an initially flat-bed channel. In-channel restoration structures are outlined in black. "rep" indicates the replicates of the experiments. Rep 1–4 are replicates with structures, while Rep 5–7 are replicates without structures. Locations s1, s2, . . ., s8 are along the channel centerline.

Table 3. Depth (mm) of Large Pools Throughout the Stream Reach in the With-Structures Replications[a]

	Location Along the Stream Meander							
Replicates	s1	s2	s3	s4	s5	s6	s7	s8
1	24.6	34.6	11.2	22.5	26.7	16.3	19.9	23.0
2	19.0	35.0	19.2	23.8	27.5	17.6	24.3	25.8
3	42.5	32.0	25.4	29.5	27.9	19.9	19.9	19.4
4	23.4	33.4	15.5	14.6	31.3	17.4	20.1	17.9
Average	27.4	33.8	17.8	22.6	28.4	17.8	21.1	21.5
SD	(9.0)	(1.2)	(5.2)	(5.3)	(1.8)	(1.3)	(1.9)	(3.1)

[a]Locations along the stream meander centerline are denoted by s1, s2,. . ., s8 and noted in Figure 6.

deepest pool (at s5) was located at the fourth J-hook (J4). The pool (at s1) upstream of the cross vane was backwater caused by the cross vane. Table 4 summarizes the average slope of large riffles created by the in-channel structures, and the water surface slope above the riffle locations. The riffle (at s5) with the steepest average slope also had the steepest water surface slope. There was no apparent trend between the riffle slope in channels with restoration structures and the riffle slope in channels without structures.

The stream channels without in-channel restoration structures did not develop a distinguishable riffle-pool sequence, but did experience severe bank erosion and sediment deposition in channel locations near s7 and s8 (Figure 6). Channels with restoration structures also experienced significant erosion and deposition at similar locations, even though J-hooks were installed along the outer bank. We compared sediment loss and sediment deposition, calculated as the volume of sediment removed from or deposited to the bank area (outlined in blue in Figure 3), downstream of the fifth J-hook (J5) in with and without-structures scenarios (Figure 7). Channels without structures experienced an average net sediment loss of 31.8 cm^3 in that bank area, while channels with structures experienced an average net sediment loss of 21.0 cm^3. Channels without structures experienced an average sediment deposition of 5.4 cm^3 in that bank area, while channels with structures experienced an average net sediment deposition of 10.0 cm^3. In-channel structures reduced sediment loss and increased sediment deposition in the stream reach, but no statistical significance ($\alpha = 0.05$) in the sediment loss or deposition between channels with and without structures ($p > 0.05$) were found in this study. The elevated stream stage, backwater and forced-morphology pools resulted in a 74% increase in the volume of the stream water in the entire stream reach, from an average of 822 to 1433 cm^3.

4. Discussion

4.1. Stream Meander Hydrology and Implications on Hyporheic Exchange

One of the main drivers of observed changes to the stream meander hydrology is the backwater that extended upstream by two or more channel widths, caused by the cross vane in-channel structure. Cross vanes act like dams that partially impede and slow streamflow with their raised structure extending across the stream channel. The backwater caused by the cross vane affected the hydraulic head gradient throughout the stream reach and the intrameander zone. The streamwise hydraulic gradient between the elevated backwater and the stream stage downstream of the cross vane can significantly induce vertical hyporheic exchange around the structure [*Crispell and Endreny*, 2009; *Daniluk et al*., 2013; *Hester and Doyle*, 2008; *Lautz and Fanelli*, 2008]. The intrameander hydraulic gradient between the elevated backwater and the nearby

Table 4. Average Gradient (and Standard Deviation) of Large Riffles and the Corresponding Water Surface (WS) at the Centerline of Channels With and Without Structures[a]

	Location Along the Stream Meander							
	s2		s5		s6		s8	
Channel Type	Riffle	WS	Riffle	WS	Riffle	WS	Riffle	WS
With Structures	0.012 (0.073)	0.023 (0.003)	0.020 (0.026)	0.024 (0.004)	0.013 (0.009)	0.016 (0.002)	0.017 (0.004)	0.018 (0.003)
No structures	−0.002 (0.003)	0.006 (0.001)	0.018 (0.005)	0.007 (0.003)	0.007 (0.003)	0.017 (0.012)	0.017 (0.011)	0.014 (0.002)

[a]Locations along the stream channel are noted in Figure 6.

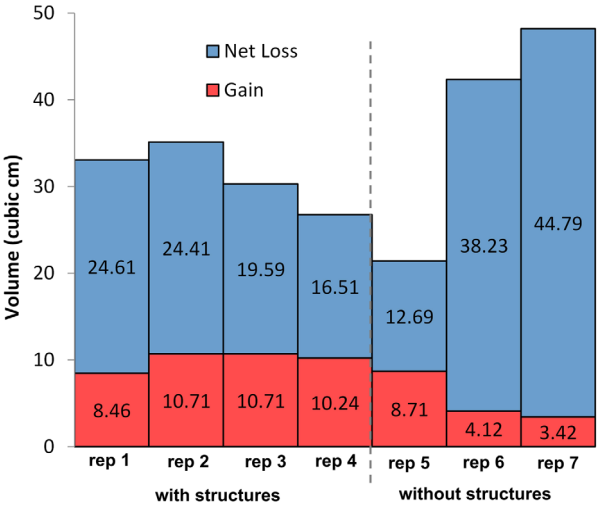

Figure 7. Erosion (net loss, blue) and deposition (gain, red) volumes at the outer bank (outlined in blue in Figure 3) downstream of the fifth J-hook (J5). Net loss is the volume of sediment removed from that bank area. Gain is the volume of sediment that was scoured from the bank and/or other areas of the channel but was deposited in that bank area. In-channel restoration structures reduced sediment loss and increased sediment deposition in the stream reach, but no statistical significance ($\alpha = 0.05$) in the sediment loss or deposition between channels with and without structures ($p > 0.05$) was found in the current study.

intrameander water table can also induce lateral hyporheic exchange into riparian areas and point bars as beaver and debris dams have been found to do [*Janzen and Westbrook*, 2011; *Jin et al*., 2009]. The elevated streamwise water surface slope in our study resulted in a statistically significant increase of ~1.0% to the intrameander hydraulic gradients across the meander neck and center (Table 4), and an increase of 2.6% (from 3.7% to 6.3%) and 4.2% (from 1.7% to 5.9%) in local hydraulic gradients next to the meander neck and center, respectively (Figure 5). While the fine sediment accumulation in backwater pools behind structures, and the subsurface boulder footers below structures, may constrain hyporheic exchange [*Lautz and Fanelli*, 2008], electrical resistivity field data found hyporheic exchange at cross vanes was spatially larger and temporally longer than at natural riffles [*Smidt et al*., 2014], suggesting macropores and steeper gradients compensate for areas with flow impediments. Stream restoration projects are increasingly evaluated for improving the ecological functions of degraded streams. Deeper flows due to backwaters might be more favorable for adult resident trout [*Vondracek and Longanecker*, 2006]. Yet less exposed gravel in the substrate and fewer riffles are likely to negatively impact trout spawning habitat, macroinvertebrate communities, and biofilm productivity [*Salant et al*., 2012]. The six J-hooks installed in this study have only one arm each that deflects flow from the outer bank. The four J-hooks at the meander apex increased the stream stage by only one third of the cross vane's impact at the meander center, and marginally changed the intrameander hydraulic gradient and water table profile at the meander apex.

The water surface profile upstream of the cross vane was flattened by the resulting backwater pool. However, the cross vane also caused a steepened water surface slope at the transition from the backwater pool to the downstream section. This steepened slope over the structure has a step-like shape, and has been observed in other stream channels with restoration structures [*Crispell and Endreny*, 2009; *Daniluk et al*., 2013; *Salant et al*., 2012] and in computational fluid dynamic simulations of structures [*Zhou and Endreny*, 2012]. The statistically significant 0.4% increase to the streamwise water surface slope in our river table "restored" stream reach is comparable to the results from a similar study comparing restored reaches to their associated reference reaches [*Daniluk et al*., 2013]. Other studies of longer restored stream reach lengths and a series of cross vanes throughout the reach also reported an increase in water surface slope after the installation of in-channel restoration structures, although the overall water surface elevations may increase [*Buchanan et al*., 2012] or not [*Salant et al*., 2012] under various flow conditions.

The in-channel restoration structures were installed at the upstream two thirds of our river table stream reach, aiming to maximize the laboratory efficiency to represent the range of possible conditions that may occur in real river restoration projects. Our values of the streamwise and intrameander hydraulic gradients represent the transitional areas where the installation of in-channel stream restoration structures stops before the end of a stream meander wavelength. Future research can install in-channel restoration structures throughout a meander wavelength or multiple meander wavelengths for evaluations of streamwise and intrameander hydraulic gradients of stream meanders in restoration projects.

4.2. Channel Morphology

The bed morphology of stream channels without in-channel restoration structures were mostly absent of a distinct riffle-pool sequence, because the stream model lacked roughness elements of natural fluvial

systems such as heterogeneous sediment mixture and vegetation. In response to the restoration structures being installed in the stream channel, streamflow created scour pools around and/or downstream of the structures, and redistributed the scour pool sediment further downstream to form riffles (Figure 4). The forced bed morphology is an indication of fluvial processes that are at work in stream reaches undergoing restoration treatments.

Cross vanes are known to create deep scour pools, which are desired for fish and wildlife habitat [*Buchanan et al*., 2012; *Endreny and Soulman*, 2011; *Rosgen*, 2006]. These scour pools are also areas of pronounced upwelling and downwelling of hyporheic flux [*Crispell and Endreny*, 2009; *Lautz and Fanelli*, 2008]. Consistently, in each experimental run in our study, the deepest scour pool was carved by streamflow going over the cross vane and dissipating its energy. The head loss at the cross vane alone accounted for 16% of total head loss in our moderate-gradient stream reach. The depth and volume of scour pools created by cross vanes were found to be generally influenced by the drop height over the cross-vane crest and the degree of bankfull width constriction through the structure [*Meyer and Bledsoe*, 2007].

The other scour pools in our stream reach were created by the four J-hooks at the stream meander apex. The development of these scour pools at the channel center was expected. J-hooks redirect the peak streamwise mass transport from the outer bank toward the center of the channel, reversing the secondary circulation flow that targets outer banks and creating recirculation eddies in the mid-channel [*Zhou and Endreny*, 2012]. However, the position of the scour pools at the hooked tip of the structures instead of downstream of the curved tip was not expected. The crest height of the J-hook tip may have been too high, which could have induced the scouring effects of the recirculation eddies at that location. The longitudinal slope of the J-hook was also designed to be higher than in real world, which may have led to higher secondary flows at the channel center around the J-hook. A study found that a majority of flow deflectors may be malfunctioning at or near a meander apex from excessive scouring [*Buchanan et al*., 2012]. As a result, the scouring effect of J-hooks installed at the meander apex needs further testing and/or simulation.

The structure-induced backwater may increase the local flow depth and enhance local erosion [*Lotsari et al*., 2014]. Although J-hooks J1 and J2 were inundated by backwater caused by the cross vane, there was obvious local erosion around J2 in comparison with the same channel bed locations in the without-structures scenarios (Figure 6). Severe bank erosion occurred downstream of the meander apex in the stream channels both with and without in-channel restoration structures. The location of the bank erosion is in accordance with the general observation that boundary shear stress peaks along the outer bank just downstream of meander apex [*Buchanan et al*., 2012]. Sediment scoured from the stream bank was deposited in the channel downstream of the scoured bank, creating a long riffle section that spanned two to three channel widths. This study showed that another in-channel flow deflection structure downstream of the meander apex would likely further minimize the bank erosion at that location.

Despite the higher local erosion, the in-channel restoration structures decreased the net erosion volume at the bank downstream of J5 by an average of 33% (each replicate is shown in Figure 7). They may have weakened the downstream secondary circulation flow that normally targets outer banks. In a study comparing measured stream bank erosion with multivariate regression model predictions, the researchers projected that in-channel restoration structures at Batavia Kill in the New York Catskills reduced bank erosion by 73.5% [*Chen et al*., 2005]. Lower bank erosion volumes and higher deposition volumes were observed in our experiments for the channels with in-channel restoration structures when compared with channels without structures, although these differences lacked statistical significance ($\alpha = 0.05$).

The characteristics of channel-forced morphology and the values of stream bank erosion in this study can be applied to evaluations of stream restoration projects involving the reconfiguration of stream channels and floodplains. High-resolution water surface and channel morphology data from this study can be used to test and improve numerical models estimating longitudinal and lateral flow fields and hyporheic exchange drivers in restored streams.

There are limitations in extending the current study to characterize how field sites would respond to restoration, and future experiments would help build more complete and representative databases. For example, unlike restoration projects at field sites, we had a relatively uniform sediment distribution, we did not shape pool and riffle bed forms below structures, and vegetation was not installed in the channel or floodplain. Due to the limitation of funding and time, our contribution was limited to address a specific set of

questions, with an emphasis on replicating the experiment multiple times to subject our experimental results to statistical analysis. Future research into the impacts of in-channel restoration structures on meandering streams might develop a flume stream model that more closely represent a natural stream with heterogeneous sediment sizes, heterogeneous bed forms, and vegetation. Future research can also adhere more strictly to the design and installation specifications of in-channel restoration structures by *Rosgen* [2006]. As shown in our work, the changes to hydraulic gradient and morphology are sensitive to the placement and combination of structures, suggesting variations in placement and combination may generate a different set of responses. Considering that real-world restoration projects are expensive and time consuming, we highly recommend that flume or sandbox river table studies be used to develop and improve numerical models before applying them to design real-world restorations.

5. Conclusions

This study performed a detailed comparison of the stream water surface and bed topography with and without in-channel restoration structures in a laboratory meandering stream reach. Results showed that in-channel restoration structures have significant impact on the streambed and water profiles in a stream meander and may change the local hyporheic flux patterns.

The in-channel restoration structures installed in this study pooled greater volumes of water and changed water surface profiles from gradually varied to rapidly varied at the crest of each structure, and steepened the hydraulic gradients laterally across the stream meander. Without in-channel structures, the hydraulic gradients at the stream meander neck were steepest due to stream planimetry and the differences in water surface elevations upstream and downstream of the meander neck. With in-channel structures, the hydraulic gradients at the cross vane and across the intrameander zone near the cross vane increased most significantly because of the backwater effect.

The addition of in-channel restoration structures resulted in an average of 33% decrease in stream bank erosion and an average of 85% increase in stream bank deposition. Despite having no statistical significance in the sediment loss or deposition between channels with structures and channels without structures, the forced morphologies that were absent from channels without structures can create different spatial patterns of surface water to groundwater gradient.

The water and streambed profile responses to in-channel restoration structures at a stream meander have implications on hyporheic exchange. Results of this study can inform the design of stream restoration projects and/or in-channel structures, such as the placement location and design of cross vanes and J-hooks. High-resolution water surface and channel morphology data from this study can also improve numerical models of the flow field and the longitudinal and lateral hyporheic exchanges in restored streams.

Acknowledgments

This research was supported by NSF EAR 09–11547. Technical assistance was provided by EmRiver staff, A. Greenhill, H. Tieu, P. Szemkow, M. Neffra, and T. Zhou. We acknowledge B. Reschke for his thoughtful construction of the river table. We also acknowledge two anonymous reviewers and the Associate Editor for their valuable comments which helped to considerably improve the quality of the manuscript. Interested readers may contact Bangshuai Han or Hong-Hanh Chu for access to the data generated in this study.

References

Abad, J., B. Rhoads, İ. Güneralp, and M. García (2008), Flow structure at different stages in a meander-bend with Bendway Weirs, *J. Hydraul. Eng.*, *134*(8), 1052–1063, doi:10.1061/(ASCE)0733-9429(2008)134:8(1052).

Bernhardt, E. S., and M. A. Palmer (2011), River restoration: The fuzzy logic of repairing reaches to reverse catchment scale degradation, *Ecol. Appl.*, *21*(6), 1926–1931, doi:10.2307/41416628.

Bernhardt, E. S., M. Palmer, J. D. Allan, G. Alexander, K. Barnas, S. Brooks, J. Carr, S. Clayton, C. Dahm, and J. Follstad-Shah (2005), Synthesizing U. S. river restoration efforts, *Science*, *308*(5722), 636–637, doi:10.1126/science.1109769.

Boano, F., C. Camporeale, R. Revelli, and L. Ridolfi (2006), Sinuosity-driven hyporheic exchange in meandering rivers, *Geophys. Res. Lett.*, *33*, L18406, doi:10.1029/2006GL027630.

Boulton, A. J., S. Findlay, P. Marmonier, E. H. Stanley, and H. M. Valett (1998), The functional significance of the hyporheic zone in streams and rivers, *Annu. Rev. Ecol. Syst.*, *29*, 59–81, doi:10.1146/annurev.ecolsys.29.1.59.

Buchanan, B. P., M. T. Walter, G. N. Nagle, and R. L. Schneider (2012), Monitoring and assessment of a river restoration project in central New York, *River Res. Appl.*, *28*(2), 216–233, doi:10.1002/rra.1453.

Cardenas, M. B., J. L. Wilson, and V. A. Zlotnik (2004), Impact of heterogeneity, bed forms, and stream curvature on subchannel hyporheic exchange, *Water Resour. Res.*, *40*, W08307, doi:10.1029/2004WR003008.

Chen, Y., S. K. Bhatia, J. Buchanan, D. DeKoskie, and R. VanSchaack (2005), Effectiveness of stream restoration in reducing stream bank erosion: The case of Batavia Kill Stream Restoration Projects, New York, paper presented at Managing Watersheds for Human and Natural Impacts, Am. Soc. of Civ. Eng., Williamsburg, Va.

Crispell, J. K., and T. A. Endreny (2009), Hyporheic exchange flow around constructed in-channel structures and implications for restoration design, *Hydrol. Processes*, *23*(8), 1158–1168, doi:10.1002/hyp.7230.

Daniluk, T. L., L. K. Lautz, R. P. Gordon, and T. A. Endreny (2013), Surface water–groundwater interaction at restored streams and associated reference reaches, *Hydrol. Processes*, *27*(25), 3730–3746, doi:10.1002/hyp.9501.

Dijk, W. M., W. I. Lageweg, and M. G. Kleinhans (2012), Experimental meandering river with chute cutoffs, *J. Geophys. Res.*, *117*, F03023, doi: 10.1029/2011JF002314.
Doll, B. A., G. L. Grabow, K. R. Hall, J. Halley, W. A. Harman, G. D. Jennings, and A. D. E. Wise (2003), *Stream Restoration: A Natural Channel Design Handbook*, 128 pp., N. C. Stream Restoration Inst., N. C. State Univ., Raleigh.
Doyle, M. W., D. Shields, K. F. Boyd, P. B. Skidmore, and D. Dominick (2007), Channel-forming discharge selection in river restoration design, *J. Hydraul. Eng.*, *7*(831), 831–837, doi:10.1061/(ASCE)0733-9429(2007)133:7(831).
Elliott, A. H., and N. H. Brooks (1997), Transfer of nonsorbing solutes to a streambed with bed forms: Laboratory experiments, *Water Resour. Res.*, *33*(1), 137–151, doi:10.1029/96WR02783.
Endreny, T. A., and K. Backer (2013), Review of fields and streams: Stream restoration, neoliberalism, and the future of environmental science, *Ecol. Restoration*, *31*(3), 339–340, doi:10.1353/ecr.2013.0049.
Endreny, T. A., and M. M. Soulman (2011), Hydraulic analysis of river training cross-vanes as part of post-restoration monitoring, *Hydrol. Earth Syst. Sci.*, *15*(7), 2119–2126, doi:10.5194/hess-15-2119-2011.
Gomez, J. D., J. L. Wilson, and M. B. Cardenas (2012), Residence time distributions in sinuosity-driven hyporheic zones and their biogeochemical effects, *Water Resour. Res.*, *48*, W09533, doi:10.1029/2012WR012180.
Gordon, R. P., L. K. Lautz, and T. L. Daniluk (2013), Spatial patterns of hyporheic exchange and biogeochemical cycling around cross-vane restoration structures: Implications for stream restoration design, *Water Resour. Res.*, *49*, 2040–2055, doi:10.1002/wrcr.20185.
Han, B., and T. A. Endreny (2013), Spatial and temporal intensification of lateral hyporheic flux in narrowing intra-meander zones, *Hydrol. Processes*, *27*(7), 989–994, doi:10.1002/hyp.9250.
Han, B., and T. A. Endreny (2014a), River surface water topography mapping at sub-millimeter resolution and precision with close range photogrammetry: Laboratory scale application, *IEEE J. Selec. Top. Appl. Earth Obs. Remote Sens.*, *7*(2), 602–608, doi:10.1109/JSTARS.2014.2298452.
Han, B., and T. A. Endreny (2014b), Detailed river stage mapping and head gradient analysis during meander cutoff in a laboratory river, *Water Resour. Res.*, *50*, 1689–1703, doi:10.1002/2013WR013580.
Hester, E. T., and M. W. Doyle (2008), In-stream geomorphic structures as drivers of hyporheic exchange, *Water Resour. Res.*, *44*, W03417, doi:10.1029/2006WR005810.
Hester, E. T., and M. N. Gooseff (2010), Moving beyond the banks: Hyporheic restoration is fundamental to restoring ecological services and functions of streams, *Environ. Sci. Technol.*, *44*(5), 1521–1525, doi:10.1021/es902988n.
Ikeda, S., G. Parker, and K. Sawai (1981), Bend theory of river meanders. Part 1. Linear development, *J. Fluid Mech.*, *112*, 363–377, doi: 10.1017/S0022112081000451.
Janzen, K., and C. J. Westbrook (2011), Hyporheic flows along a Channelled Peatland: Influence of Beaver Dams, *Can. Water Resour. J.*, *36*(4), 331–347, doi:10.4296/cwrj3604846.
Jenkinson, R. G., K. A. Barnas, J. H. Braatne, E. S. Bernhardt, M. A. Palmer, and J. D. Allan (2006), Stream restoration databases and case studies: A guide to information resources and their utility in advancing the science and practice of restoration, *Restoration Ecol.*, *14*(2), 177–186, doi:10.1111/j.1526-100X.2006.00119.x.
Jin, L., D. I. Siegel, L. K. Lautz, and M. H. Otz (2009), Transient storage and downstream solute transport in nested stream reaches affected by beaver dams, *Hydrol. Processes*, *23*(17), 2438–2449, doi:10.1002/hyp.7359.
Kasahara, T., and S. M. Wondzell (2003), Geomorphic controls on hyporheic exchange flow in mountain streams, *Water Resour. Res.*, *39*(1), 1005, doi:10.1029/2002WR001386.
Kondolf, G. M., and E. R. Micheli (1995), Evaluating stream restoration projects, *Environ. Manage.*, *19*(1), 1–15, doi:10.1007/BF02471999.
Lautz, L. K., and R. M. Fanelli (2008), Seasonal biogeochemical hotspots in the streambed around restoration structures, *Biogeochemistry*, *91*(1), 85–104, doi:10.1007/s10533-008-9235-2v.
Lave, R. (2009), The controversy over natural channel design: Substantive explanations and potential avenues for resolution, *J. Am. Water Resour. Assoc.*, *45*(6), 1519–1532, doi:10.1111/j.1752-1688.2009.00385.x.
Lehr, C., F. Pöschke, J. Lewandowski, and G. Lischeid (2015), A novel method to evaluate the effect of a stream restoration on the spatial pattern of hydraulic connection of stream and groundwater, *J. Hydrol.*, *527*, 394–401, doi:10.1016/j.jhydrol.2015.04.075.
Lotsari, E., M. Vaaja, C. Flener, H. Kaartinen, A. Kukko, E. Kasvi, H. Hyyppä, J. Hyyppä, and P. Alho (2014), Annual bank and point bar morphodynamics of a meandering river determined by high-accuracy multitemporal laser scanning and flow data, *Water Resour. Res.*, *50*, 5532–5559, doi:10.1002/2013WR014106.
Meyer, J. E., and B. P. Bledsoe (2007), Restoration structure inventory and survey results from the Little Snake River and tributaries, Northern Colorado, PhD dissertation, Colo. State Univ., Fort Collins.
Packman, A. I., and N. H. Brooks (2001), Hyporheic exchange of solutes and colloids with moving bed forms, *Water Resour. Res.*, *37*(10), 2591–2605, doi:10.1029/2001WR000477.
Palmer, M. A., et al. (2005), Standards for ecologically successful river restoration, *J. Appl. Ecol.*, *42*(2), 208–217, doi:10.1111/j.1365-2664.2005.01004.x.
Parker, G. (1976), On the cause and characteristic scales of meandering and braiding in rivers, *J. Fluid Mech.*, *76*(03), 457–480, doi:10.1017/S0022112076000748.
Peakall, J., P. Ashworth, and J. Best (1996), Physical modelling in fluvial geomorphology: Principles, applications and unresolved issues, in *The Scientific Nature of Geomorphology*, pp. 221–253, Wiley & Sons, Chichester, U. K., doi:10.1.1.469.5288.
Radspinner, R. R., P. Diplas, A. F. Lightbody, and F. Sotiropoulos (2010), River training and ecological enhancement potential using in-stream structures, *J. Hydraul. Eng.*, *136*(12), 967–980, doi:10.1061/(ASCE)HY.1943-7900.0000260.
Revelli, R., F. Boano, C. Camporeale, and L. Ridolfi (2008), Intra-meander hyporheic flow in alluvial rivers, *Water Resour. Res.*, *44*, W12428, doi:10.1029/2008WR007081.
Rosgen, D. L. (1994), A classification of natural rivers, *Catena*, *22*(3), 169–199, doi:10.1016/0341-8162(94)90001-9.
Rosgen, D. L. (2006), *The Cross-Vane, W-Weir, and J-Hook Vane Structures. Description, Design and Application for Stream Stabilization and River Restoration*, Wildland Hydrol. Inc., Pagosa Springs, Colo., doi:10.1061/40581(2001)72. [Available at http://www. wildlandhydrology.-com.] [Updated 2006.]
Rosgen, D. L. (2011), Natural channel design: Fundamental concepts, assumptions, and methods, in *Stream Restoration in Dynamic Fluvial Systems*, pp. 69–93, AGU, Washington, D. C., doi:10.1029/2010GM000990.
Salant, N. L., J. C. Schmidt, P. Budy, and P. R. Wilcock (2012), Unintended consequences of restoration: Loss of riffles and gravel substrates following weir installation, *J. Environ. Manage.*, *109*, 154–163, doi:10.1016/j.jenvman.2012.05.013.
Schumm, S. A., and H. R. Khan (1972), Experimental study of channel patterns, *Geol. Soc. Am. Bull.*, *83*(6), 1755–1770, doi:10.1130/0016-7606(1972)83[1755:ESOCP]2.0.CO;2.

Simon, A., M. Doyle, M. Kondolf, F. D. Shields, B. Rhoads, and M. McPhillips (2007), Critical evaluation of how the Rosgen classification and associated "Natural Channel Design" methods fail to integrate and quantify fluvial processes and channel response, *J. Am. Water Resour. Assoc.*, *43*(5), 1117–1131, doi:10.1111/j.1752-1688.2007.00091.x.

Small, M. J., and M. W. Doyle (2011), Historical perspectives on river restoration design in the USA, *Prog. Phys. Geogr.*, *36*, 138–153, doi:10.1177/0309133311425400.

Smidt, S. J., J. A. Cullin, A. S. Ward, J. Robinson, M. A. Zimmer, L. K. Lautz, and T. A. Endreny (2014), A comparison of hyporheic transport at a cross-vane structure and natural riffle, *Ground Water*, *53*, 859–871, doi:10.1111/gwat.12288.

Smith, C. E. (1998), Modeling high sinuosity meanders in a small flume, *Geomorphology*, *25*(1), 19–30, doi:10.1016/S0169-555X(98)00029-4.

Stanford, J. A., and J. V. Ward (1988), The hyporheic habitat of river ecosystems, *Nature*, *335*, 64–66, doi:10.1038/335064a0.

Vondracek, B., and D. R. Longanecker (2006), Habitat selection by rainbow trout Oncorhynchus mykiss in a California stream: Implications for the instream flow incremental methodology, *Ecol. Freshwater Fish.*, *2*(4), 173–186, doi:10.1111/j.1600-0633.1993.tb00100.x.

Wu, W. (2008), *Computational River Dynamics*, 494 pp., CRC Press, Taylor & Francis, London, U. K.

Zhou, T., and T. Endreny (2012), Meander hydrodynamics initiated by river restoration deflectors, *Hydrol. Processes*, *26*(22), 3378–3392, doi:10.1002/hyp.8352.

Zimmer, M. A., and L. K. Lautz (2015), Pre- and post-restoration assessment of stream-ground water interactions: Impacts on hydrological and chemical heterogeneity in the hyporheic zone, *Freshwater Sci.*, *34*(1), 287–300, doi:10.1086/679514.

Zolezzi, G., and G. Seminara (2001), Downstream and upstream influence in river meandering. Part 1. General theory and application to overdeepening, *J. Fluid Mech.*, *438*, 183–211, doi:10.1017/S002211200100427X.